Analytical Verification

Introduction and Identification

In this section, the analytical models are used to verify the experimental results. The fiber element inelastic analysis was conducted and compared with the experimental results. Hysteretic behaviour responses were analyzed by TDAP3 program. The structural model was a cantilever column having elastic rotation spring and plastic hinge zone idealized by fiber elements as shown in figure 84. Inelastic material behaviour was used for this analysis. The cyclic load was applied by displacement controlled and subjected by constant axial load. The calculated stress and strain of concrete element and steel reinforcement, reaction and displacement are presented and compared. The plastic hinge length of reinforced concrete members are calculated based on Paulay and Priestley (1992). This expression is given by Equation (42).

$$l_p = 0.08l + 0.022 d_b f_y \qquad (42)$$

The plastic hinge length of test specimens as following

$$l_p = 0.08 \times 1.55 + 0.022 \times 0.013 \times 395 \quad = \quad 0.24 \text{ m}$$

For the core concrete, the stress vs. strain model of confined concrete was idealized based on Hoshikuma et al. (1997) model and Equation (13). The stress vs. strain model of vertical reinforcement was idealized based on Menegotto and Pinto (1973) model determined as Equation (15).

The volume ratio of confinement is calculated as following:

ρ_v = ratio of confinement steel volume and core concrete volume

$$\rho_v = \frac{4A_{sh}}{ds}$$

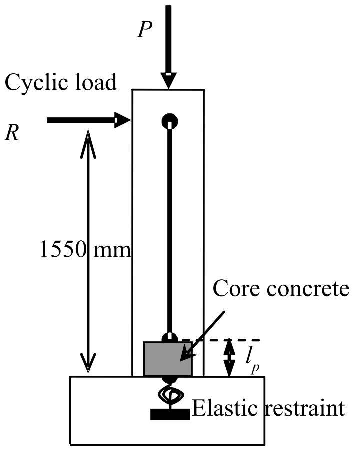

Figure 84 Analytical model

Verification of Cyclic Behavior

The peak stress and concrete stiffness of confined concrete depending on the volumetric confinement ratio were calculated as shown in Table 6.

Table 6 Peak stress of confine concrete

Specimens	f_{co} (MPa)	d (mm)	s (mm)	ρ_v	f_{cc} (MPa)	E_{des} (MPa)	ε_{cc}	ε_{cu}
A1, A2	32.36	340	50	0.0075	33.69	6418	0.0027	0.0054
B1, B2	29.61	170	100	0.0093	31.28	4299	0.0030	0.0067
C1	32.36	340	200	0.0019	32.69	25672	0.0022	0.0028
D1	29.61	170	150	0.0050	30.50	8060	0.0025	0.0044

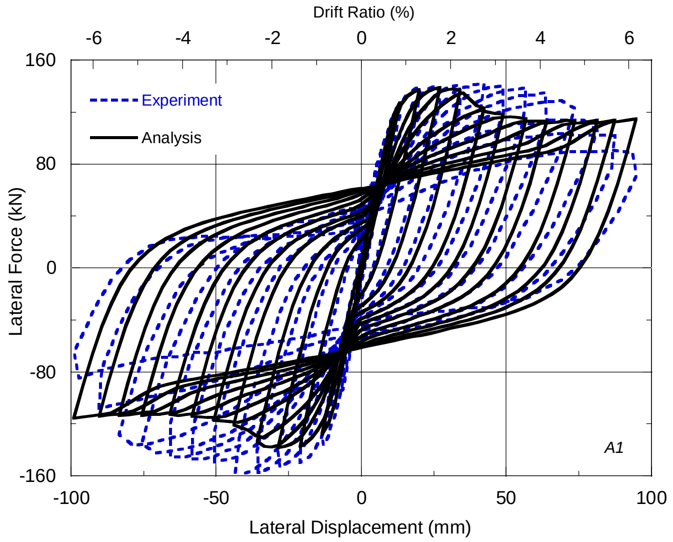

a.) Specimen A1

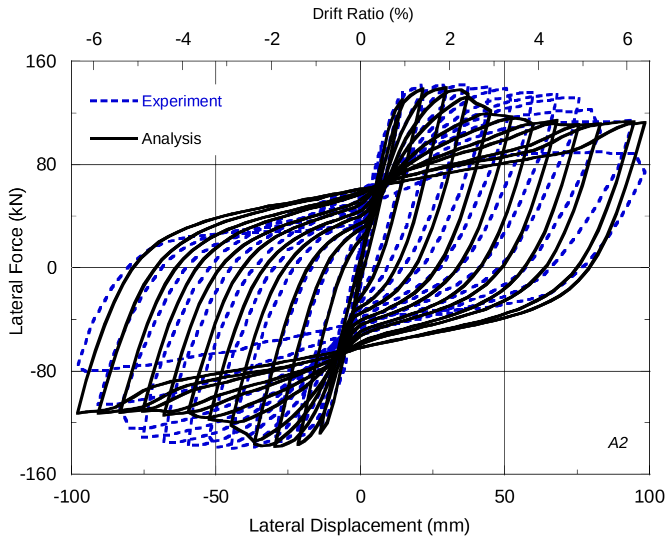

b.) Specimen A2

Figure 85 Comparison of lateral force vs. lateral displacement hytereses between analysis and experiment

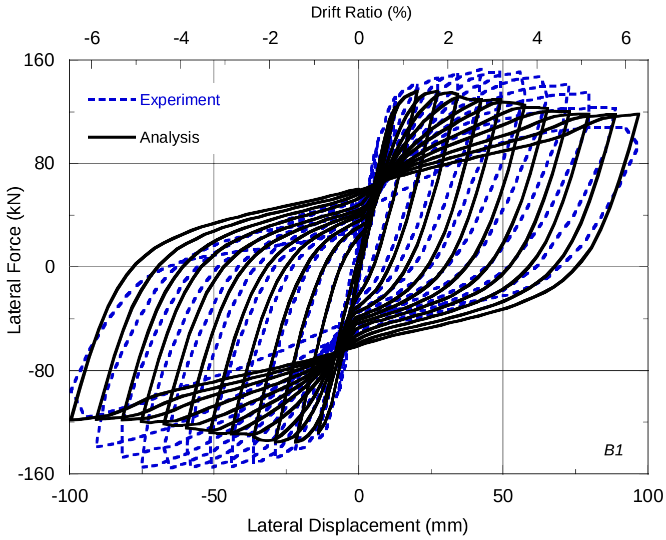

c.) Specimen B1

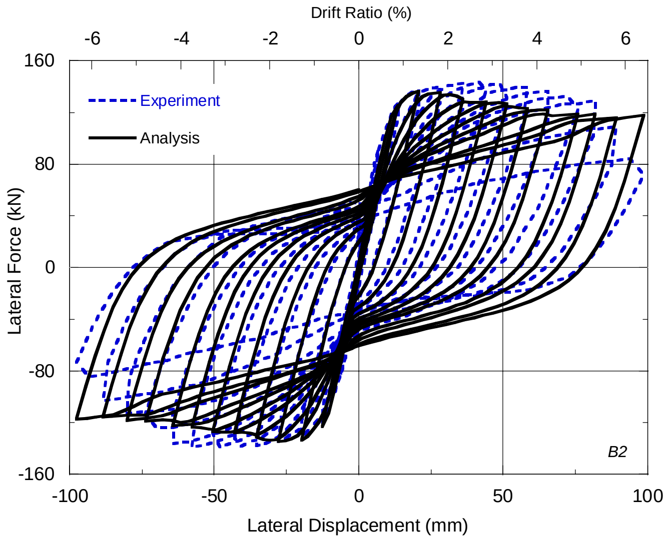

d.) Specimen B2

Figure 85 (Continued)

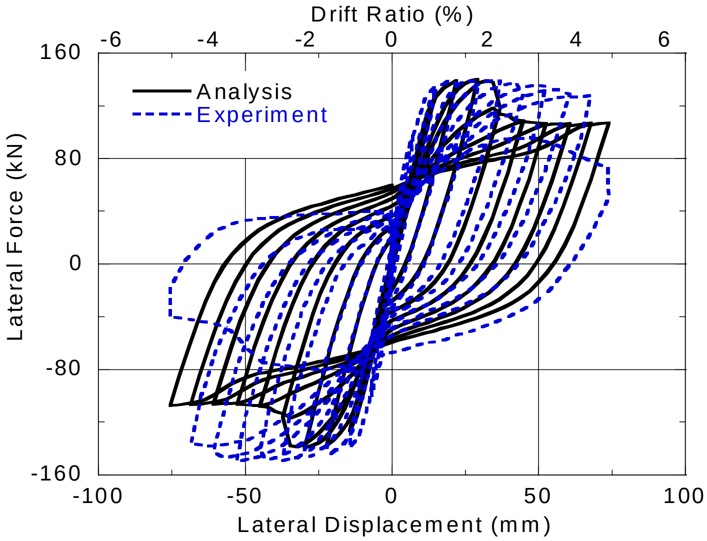

e.) Specimen C1

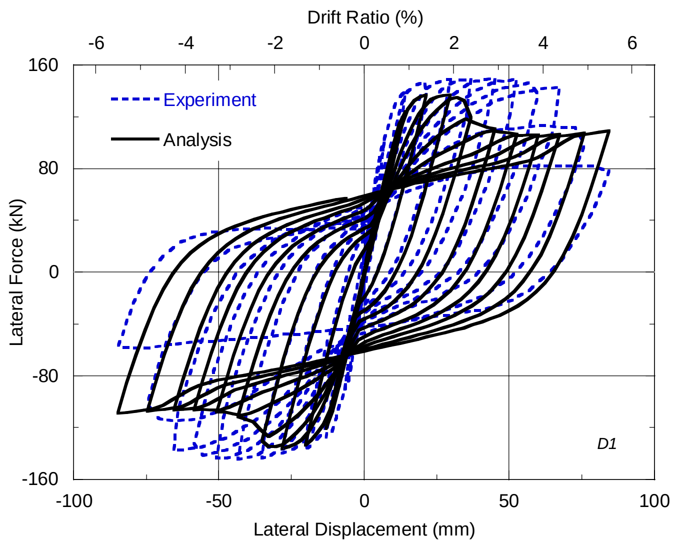

f.) Specimen D1

Figure 85 (Continued)

Fig. 85 presents the comparisons between analysis and experimental results of lateral force vs. lateral displacement hytereses.

<u>Stress and Strain behaviour of confined concrete</u>

In the analytical results, calculated stress and strain of the core concrete and the covering concrete at the extreme fiber are present in Fig. 92 through Fig. 97. Since the effect of local buckling and rupture of axial steel bars is not in considered in the fiber element analysis, the hystereses after 4% drift are not accurately predicted.

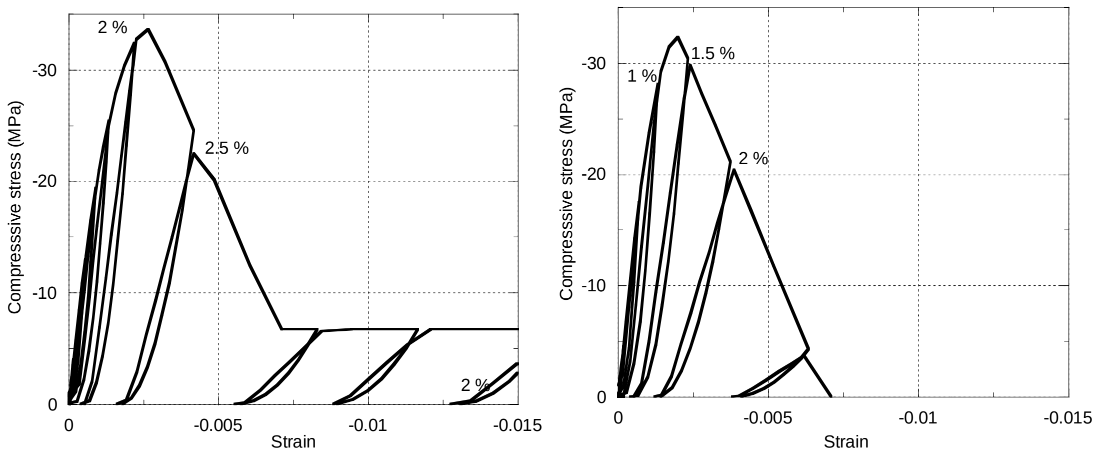

a.) Core concrete b.) Covering concrete

<u>Figure 86</u> Computed stress vs. strain hystereses of specimen A1

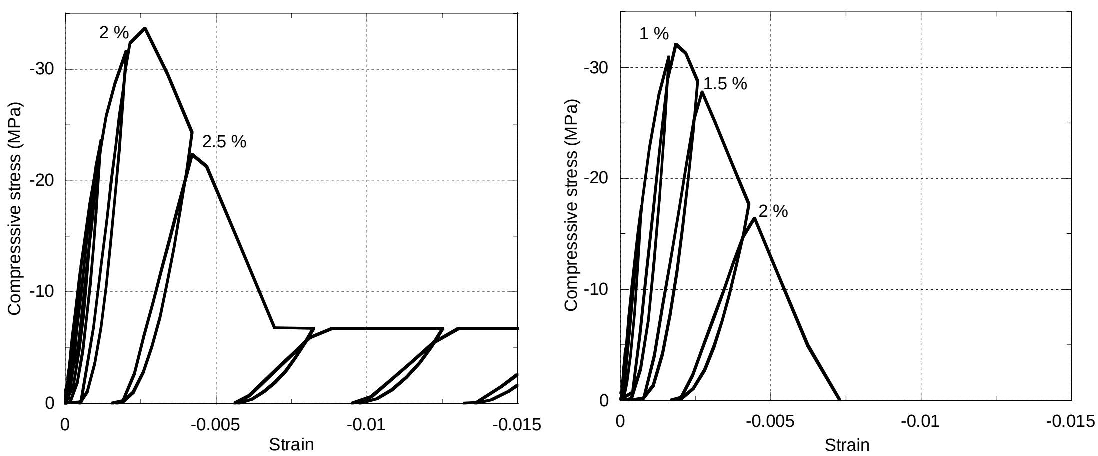

a.) Core concrete b.) Covering concrete

<u>Figure 87</u> Computed stress vs. strain hystereses of specimen A2

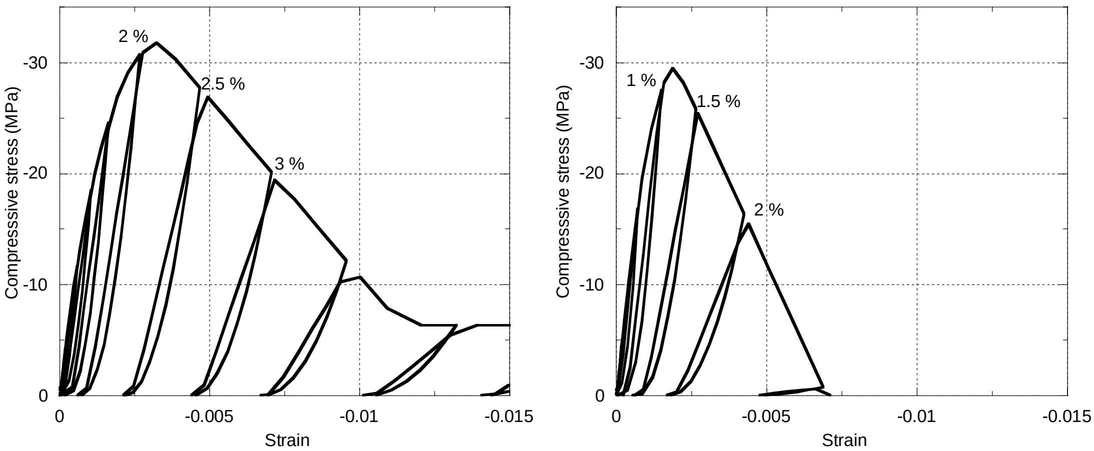

a.) Core concrete b.) Covering concrete

Figure 88 Computed stress vs. strain hystereses of specimen B1

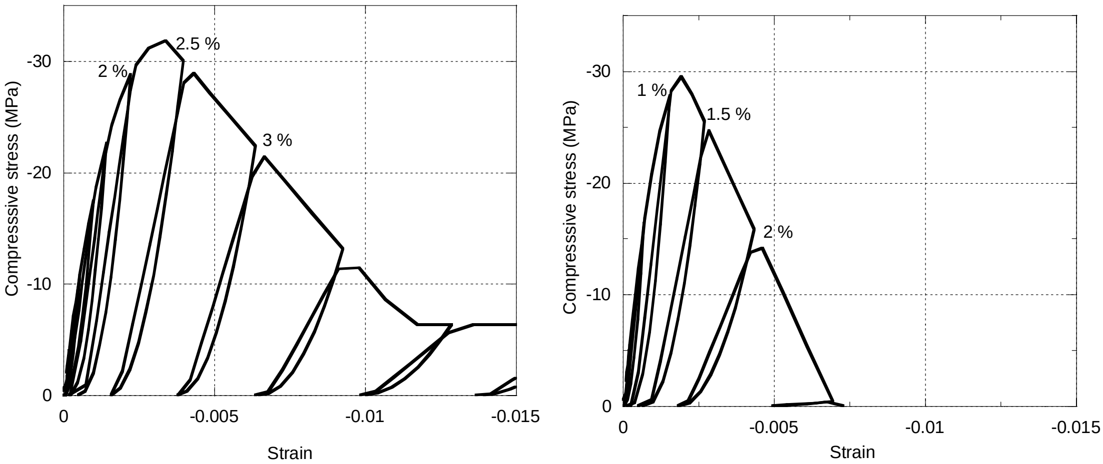

a.) Core concrete b.) Covering concrete

Figure 89 Computed stress vs. strain hystereses of specimen B2

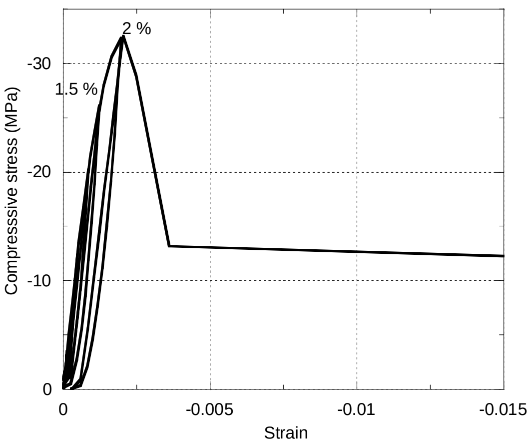

a.) Core Concrete

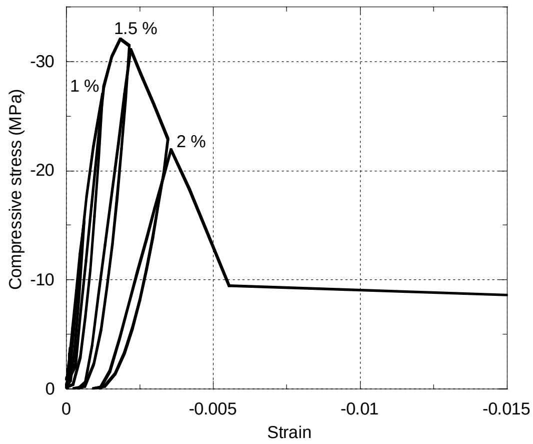

b.) Covering Concrete

Figure 90 Computed stress vs. strain hystereses of specimen C1

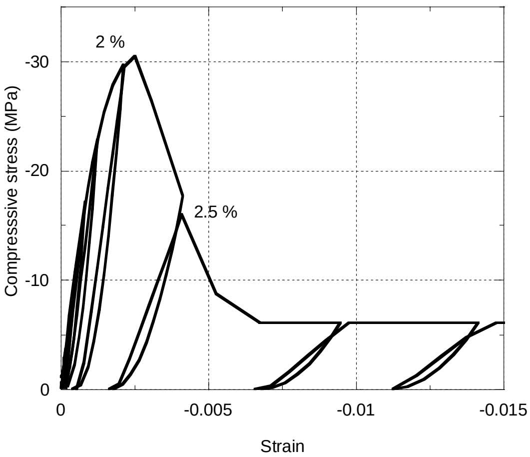

a.) Core concrete

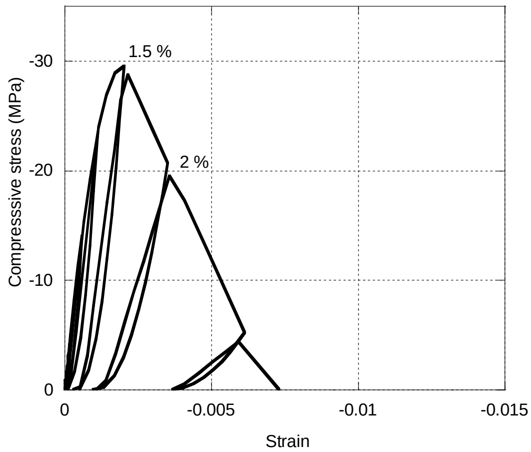

b.) Covering concrete

Figure 91 Computed stress vs. strain hystereses of specimen D1

The maximum displacement, Δ_{u1} (column 5 of table 7) was determined when the lateral force was unloaded to 75% of R_{max} (Wehbe et al. 1999). The mode of failure at the end of the tests of specimens A1, A2, B1, B2 and D1 is flexural failure while that of specimen C1 being flexural-shear failure. The maximum displacement was determined when the lateral force capacity was reduced to 75% of P_{max}.

On the other hand, when the compressive stress in core concrete on the descending branch was beyond 50% of the core concrete peak stress ($f^{'}_{cc}$), crushing of core concrete and bucking of longitudinal reinforcement occurred. According to Hoshikuma et al., (1997) criteria of the column failure and maximum displacement, Δ_{u2} was defined when the stress of core concrete on the descending branch reached 50% of $f^{'}_{cc}$. The analytical results of cyclic lateral force and displacement is shown in Table 7. The axial strain at 50% of $f^{'}_{cc}$ was used to observe Δ_{u2} of the specimens in the experiments. For each specimen, the lateral strain in concrete core at failure is the axial strain times the Poisson ratio of 0.2. This is also the strain in the tie bars and the drift ratios can be recorded. The ultimate strain of concrete and measured strain record are as shown in Appendix Fig. 8.

Table 7 **Comparison of lateral force and displacement between the analysis and experiment**

	Experiment							Analytical verification			
Type	R_Y (kN)	Δ_y (mm)	R_{max} (kN)	Δ_{u1} (mm) at 75% of R_{max}	Δ_{u2} (mm)	Accumulate Dissipated Energy (kN-m)	Failure mode	R_y (kN)	Δ_y (mm)	R_{max} (kN)	Δ_u (mm)
A-1	124.49	11.75	151.76	85.07	70.2	128.64	Flexural	105.51	12.56	137.16	37.37
A-2	121.13	12.19	141.11	89.36	51.25	134.75	Flexural	89.7	10.22	137.00	34.88
B-1	121.17	10.40	154.10	92.45	79.5	135.51	Flexural	104.4	12.62	134.75	49.83
B-2	113.10	10.66	141.23	85.78	56.93	123.40	Flexural	86.36	10.05	134.53	31.33
C-1	132.41	13.51	144.52	69.97	46.5	77.64	Flexural-shear	107.62	12.33	137.95	31.75
D-1	126.95	11.04	147.16	73.70	54.25	91.14	Flexural	106.99	12.83	135.34	31.56

96

<u>Discussion on Experimental results and Verification</u>

In this research, the ultimate condition was defined by two conditions as following;

1) The maximum displacement, Δ_{u1} (column 5 of table 7) was determined when the lateral force was reduced 75% of R_{max} (Wehbe et al. 1999).

2) Based on Hoshikuma et al. (1997) criterion, when the compressive stress in core concrete on the descending branch was beyond 50% of the core concrete peak stress (f'_{cc}), crushing of core concrete and bucking of longitudinal reinforcement occurred. The column failure and maximum displacement, Δ_{u2} was defined when the stress of core concrete on the descending branch reached 50% of f'_{cc}. The axial strain at 50% of f'_{cc} was used to observe Δ_{u2} of the specimens in the experiments. For each specimen, the lateral strain in concrete core at failure is the axial strain times the Poisson ratio of 0.2. This is also the strain in the tie bars and the drift ratios can be recorded.

3) The analytical results appear to underestimate the experimental results shown in Table 7 especially in predicting the ultimate displacement. The calculated displacement is highly sensitive to the plastic hinge length. Since the effect of local buckling of longitudinal bars is not included in the analysis, the hystereses after 4% drift are not accurately predicted. The analysis results of specimens A1 A2 B2 were close to experimental results in cyclic load of 1% 1.5% and 2% drift ratio. For specimen B1, the experimental result analysis is more than analysis result in cyclic load between 2% to 5%. From experimental result, the maximum moment of all specimens shows little difference. The amount of confinement steel is less significant in flexural strength. It can be observed that the analytical behaviour is in reasonable agreement with experimental results.

In this research, it can be found that the effect to response behavior of columns subjected to cyclic load is as following:

Effect of Eccentric Load

1. Typical failure modes are similar and the dissipation energy of specimens subjected to eccentric axial loads is not significantly different from those specimens when the axial loads were concentric.
2. As shown in hysteretic loops in Fig. 98, the eccentric load was case reducing the horizontal force capacity in specimen B-1 which is less torsion rigidity.

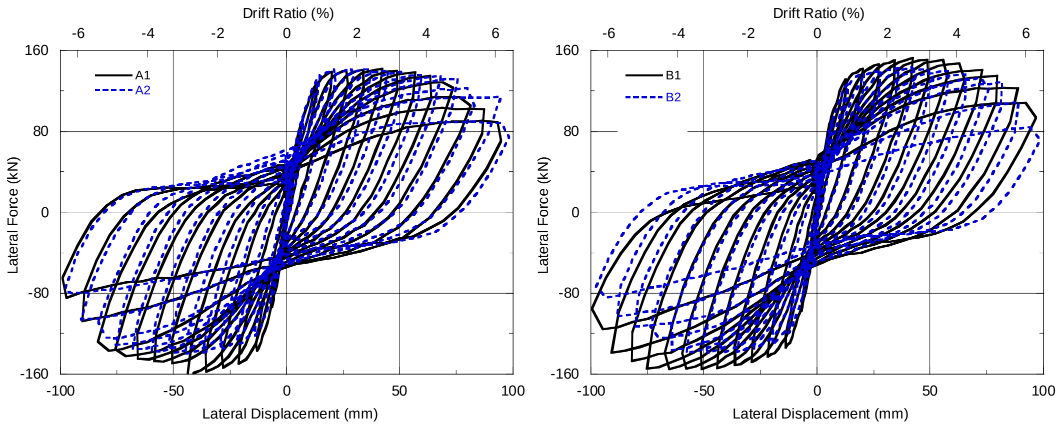

a.) Specimen A1 and A2 b.) Specimen B1 and B2

Figure 92 Comparison of lateral force vs. lateral displacement hytereses between specimens A1 and A2 and specimens B1 and B2

Effect of Cross Tie Bars

1. The effectiveness of cross ties was apparent by hysteretic loops shape developed after yield strength exceeded in specimen A1 and B1.
2. Cross ties bars can improve the maximum horizontal force capacity and ductility and can reduce damage of core concrete crushed.
3. The embedment length of longitudinal bars was located by spacing of tie reinforcement. Although the spacing of tie reinforcement is increased in specimen B-1 and B-2, it still can severe the outward buckling shape of longitudinal reinforcement by cross ties reinforced.

Therefore the effectiveness of confining tie bars was reduced by tie reinforcement without braced cross tie bars.

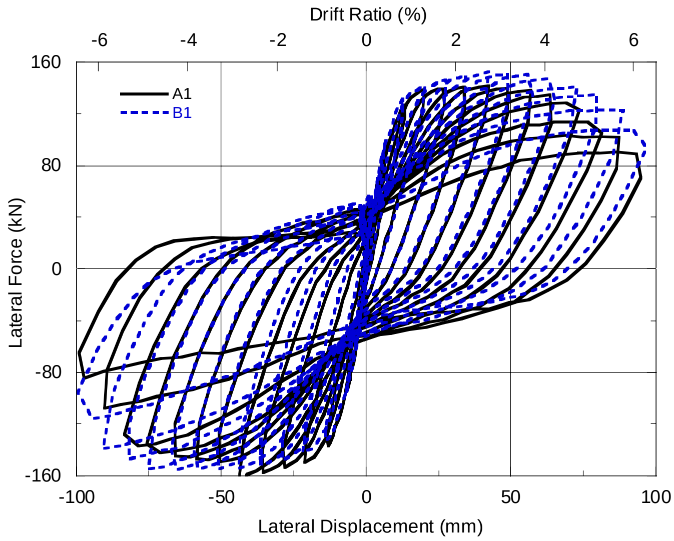

Figure 93 Comparison of lateral force vs. lateral displacement hytereses between specimens A1 and B1

Effect of Tie Reinforcement Ratio

1. Increasing the amount of tie bars does not affect the maximum lateral load force and the yield lateral force
2. Increasing the amount of tie bars increases the maximum deflection and dissipation energy of the specimens
3. In specimen C-1 in which there is low confinement, after the maximum horizontal force was reached, diagonal shear cracks appeared and brittle flexural-shear failure followed.
4. The severely damaged zone relates to the arrangement and spacing of tie bars. It increased to 43 cm from the base in specimen C-1.

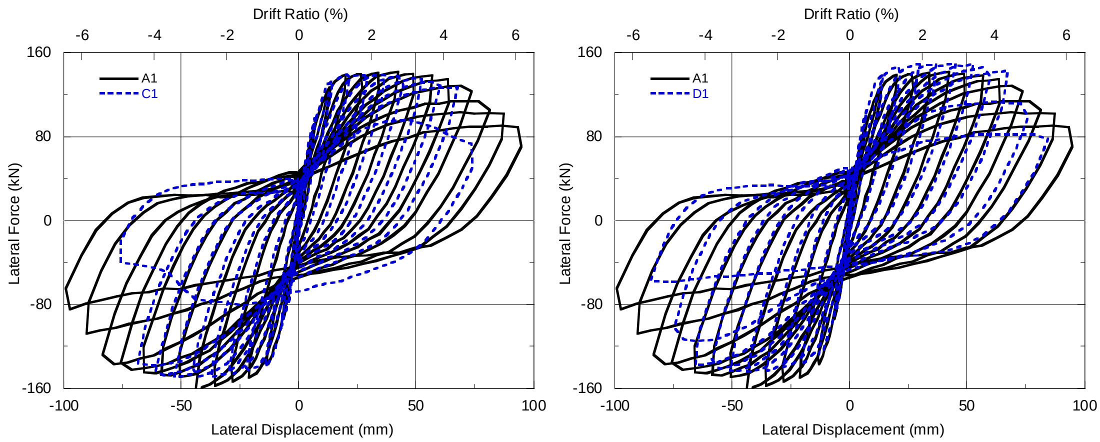

a.) Specimen A1 and C1

b.) Specimen A1 and D1

Figure 94 Comparison of the lateral force vs. lateral displacement hytereses between specimens A1, C1 and specimens A1 and D1